

Free and forced motion in an asymmetric liquid-column oscillator

BY M. J. SMITH^{1,†}, J. J. KOBINE^{1,*} AND F. A. DAVIDSON²

¹*Division of Civil Engineering, and* ²*Division of Mathematics,
University of Dundee, Dundee DD1 4HN, UK*

The results of a combined theoretical, numerical and experimental study of liquid oscillations in an asymmetric U-tube are presented. The configuration under investigation is analogous to that of the tuned liquid-column damper used to suppress oscillatory motion in large semi-supported structures. The liquid motion is described by a second-order ordinary differential equation that is nonlinear when the widths of the two vertical columns are unequal. It is shown that this asymmetry can be used as a tuning parameter to determine the natural frequency of free oscillations in the system, in addition to the known tuning effect of the connecting chamber height. The effects of viscous damping and periodic forcing are considered, leading to a description of probable initial and long-term resonance behaviour in a practical asymmetric device.

Keywords: structural damping; tuning; perturbation analysis; nonlinear resonance

1. Introduction

Advances in technology allow tall buildings and other large-scale structures to be built from light, flexible materials with relatively low levels of intrinsic damping. Consequently, the structural vibrations resulting from natural forces are far more serious, resulting in occupant discomfort, malfunction of equipment and possible structural failure. The vibrations are reduced if the stiffness of the building is increased. Traditionally, additional strength was achieved through adding more mass to the structure. However, this often resulted in aesthetic and financial inefficiency.

The dynamic response of a tall building depends on its ability to dissipate energy. For the tallest buildings, the intrinsic structural damping is insufficient to limit its motion. An effective method of absorbing and dissipating the additional energy is through the use of auxiliary damping devices. These are large substructures that are built high up or on top of the building where the motion has the greatest amplitude. The damping systems are designed to counteract the oscillatory motion of the building with their own momentum. The first auxiliary damping systems were developed in New Zealand in the early 1970s, and a comprehensive review of their implementation throughout the world is given by Holmes (1995). The development of auxiliary damping systems is currently a highly active area of research in engineering.

* Author for correspondence (j.kobine@dundee.ac.uk).

† Present address: Deepsea Engineering, Bradford House, East Street, Epsom KT17 1BL, UK.

The most regularly occurring source of excitation for a tall building is from high winds. The strength of the wind load is dependent upon the geometry of the building and the topology of the local environment. The surrounding terrain produces drag and creates a boundary-layer effect, making the tallest buildings particularly vulnerable (Plate & Kiefer 2001). Owing to the turbulent nature of wind velocities during storms, the loads acting on structures fluctuate. The response of tall buildings to high winds is discussed extensively by Holmes (2001). The role of height in a building's response becomes further apparent when comparisons are made with the work of Tamura *et al.* (2001a), which considers the response of low-rise structures to wind loading.

The forces detailed above all result in the oscillatory motion in tall buildings. Despite the fluctuations in these forces that have been discussed, it is widely accepted that when describing the driving force in an auxiliary damping system, the response can be modelled mathematically with a sinusoidal or co-sinusoidal function (e.g. Kwok *et al.* 1991). The motion of a television tower is also modelled in this manner by Hitchcock *et al.* (1997a). The tower is excited by human movement synchronized with its natural frequency and allowed to decay freely from a given amplitude. Another example of sinusoidal forcing is given by Kwok *et al.* (1997) where a steady external load is considered. The oscillatory motion along each axis is generally considered separate although bi-directional motion is also discussed by Hitchcock *et al.* (1997b). As the detail of the external force is not the main subject of this paper, a co-sinusoidal forcing function with constant amplitude is used throughout.

The damping systems can be categorized as either passive or active. Passive systems absorb energy from the initial impact and use it to counteract the movement of the primary structure through motion of a solid or liquid mass. Passive systems are relatively simple and inexpensive to build. Furthermore, they require little maintenance and no power input to operate; energy is dissipated by means of frictional effects. The early designs of passive damping systems were not adjustable to changing external loads. However, this is now possible in the modern models and such systems are often referred to as 'semi-active'. Active dampers rely on mechanically generated energy to counteract the building motion. They are adjustable to a change in loading and are controlled by sensors throughout the building. The mechanical input means that they are relatively expensive and complicated to build and a large power supply is required. A good overview of damping systems is given by Tamura (1998), and further examples of active control devices are discussed by Ribakov *et al.* (2001) and Chen & Scawthorn (2003).

A tuned sloshing damper (TSD) is the simplest form of a liquid-based damping system. It relies on the liquid motion in a rigid container to absorb and dissipate vibrational energy. Dissipation is primarily achieved through wave breaking on the free surface. Systems of this type have already been successfully installed in practice and are discussed further by Holmes (2001). The natural frequency of a TSD can only be controlled by adjusting the fluid depth, since the dimensions of the tank are fixed. Recent work by Sakamoto *et al.* (2001) also describes controlling the natural frequency of a TSD by applying an electric field to an electrorheological fluid.

A tuned liquid-column damper (TLCD) is a modified design of a TSD. It comprises two vertical columns that are joined at the base by a horizontal chamber, forming the shape of a U-tube. The liquid (usually water) oscillates

predominantly vertically within the columns due to gravity and horizontally in the connecting chamber. It is the momentum of the latter flow that counteracts the motion of the building. The width of the device in the crossflow direction is normally sufficient to allow the oscillating flow to be considered as two dimensional in the vertical and streamwise horizontal directions. Energy is lost through friction generated by orifices or turbines in the horizontal chamber. A TLCDC is inexpensive to install and requires little maintenance. Furthermore, existing water tanks on tall buildings can be modified to act as a TLCDC and provide additional damping. A large volume of water on top of a building can also be used for everyday purposes and is a useful source for fire-fighters.

Analogous systems known as stabilizers are used in cargo ships to reduce the rolling motion caused by waves. The initial models were simple rectangular tanks filled with liquid, which were similar to the TSD model. A U-shaped design was later proposed by [Field & Martin \(1976\)](#). There, the configuration of the tanks is discussed in detail before experimental test results are presented. The benefits and the practicalities of both systems are also discussed.

The initial design of the TLCDC considers a U-tube with a constant cross-sectional area and is discussed by [Xu *et al.* \(1992\)](#). In this case, the natural frequency is adjusted by varying the volume of fluid in the tank. The design was modified by [Hitchcock *et al.* \(1997a\)](#) to describe symmetric vertical columns connected by a horizontal chamber of variable height. This allows greater versatility as the natural frequency can be controlled by the geometry of the tank rather than just the volume of fluid. Work by [Gao *et al.* \(1999\)](#) gives a theoretical analysis of systems of more than one TLCDC with natural frequencies distributed around the natural frequency of the building. This latter technique results in the system being less sensitive to changes in external loading.

In this paper, a study of liquid oscillations in a generalized U-tube with a variable horizontal chamber and column widths is presented. The liquid oscillations in an asymmetric U-tube were first discussed by [Bernoulli \(1738\)](#). Through a geometrical model, Bernoulli calculated the length of a pendulum that would have identical frequency to the oscillations in an asymmetric U-tube. His work concluded that as the asymmetry is increased the length of the isochronous pendulum becomes shorter and it will oscillate faster. There has apparently been no further detailed discussion of this problem until now.

2. Theoretical analysis

(a) Formulation

A generalized U-tube is considered as shown in [figure 1](#). The fundamental assumption that is made in formulating the theoretical model is that the global flow can be treated as two dimensional, with the velocity component perpendicular to the diagrammatic plane being equal to zero. This assumption is motivated by the characteristics of TLCDC devices, which are generally designed with a uniform cross-section in one horizontal direction and are aligned so as to move predominantly in the perpendicular horizontal direction.

The height of the horizontal chamber and the widths of the left and right columns are denoted by r'_b , and r'_1 and r'_2 , respectively (the dash indicates that the quantities are dimensional). It is assumed that $r'_1 \geq r'_2$. At equilibrium, the

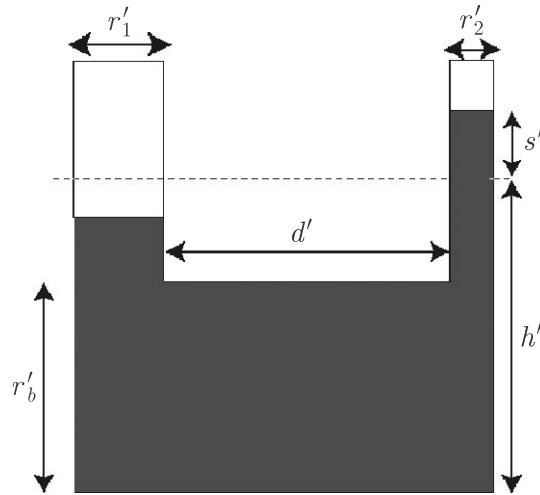


Figure 1. Schematic of the two-dimensional cross-section of a liquid-column oscillator.

liquid fills both columns to a height h' above the base. When oscillating under the influence of gravity, the maximum amplitude in the narrower column is denoted by S'_{\max} . It is assumed that the columns are sufficiently tall to accommodate the maximum vertical extent of such oscillations. It is further assumed that $|S'_{\max}| < h' - r'_b$, so that both columns are always at least partially full.

The geometry of the problem is such that it is impractical to seek an analytical solution of the two-dimensional, time-dependent Navier–Stokes equations. Even neglecting viscous effects and thereby reducing the governing equations to the time-dependent Euler equations does not simplify the modelling challenges sufficiently to allow elucidation of a global velocity field that respects such features as the oscillating free surfaces and the corner effects. Instead, we adopt an energy and flux-conserving Lagrangian approach that was used successfully by Craik & Hirata (2003) to model liquid oscillations in a conceptual configuration of three vertical cylinders connected at their bases. Thus we deem the local flow in each of the three parallel-sided sections of our device to be unidirectional and parallel to the boundaries. All non-parallel motion is therefore assumed to be limited to the corner regions. Given that these have a total area not exceeding 25% of the total cross-sectional area, the unidirectional parallel approximation can legitimately be extended to the entire flow domain. Furthermore, we treat the liquid motion as being inviscid, which is to say that the internal widths of the geometry shown in figure 1 are much greater than the length scales associated with the viscous boundary layers in the flow. It will be seen in §4 that these assumptions are valid when the predictions of the theoretical model are compared with the results of laboratory experiments.

An equation describing the oscillations is derived in terms of the upward displacement of the liquid–air interface in the columns, denoted by $s'_j(t')$ ($j=1, 2$) where t' denotes time. Displacement and time are non-dimensionalized as

$$s_j(t) = \frac{s'_j(t')}{h'}, \quad t = t' \sqrt{\frac{g}{h'}}$$

where g represents acceleration due to gravity. The parameters d' , r'_1 , r'_2 and r'_b are non-dimensionalized by division by h' .

The governing equations of motion can be derived from Bernoulli's equation for time-dependent flow. However, a more elegant and direct method is to construct the Lagrangian of the motion and apply Lagrange's equations (e.g. Kibble & Berkshire 2004). If the zero level of potential energy is taken to be when the fluid is at rest with $s_1 = s_2 = 0$, then the dimensionless potential energy V of the displaced fluid is given by

$$V = \frac{1}{2}(r_1 s_1^2 + r_2 s_2^2).$$

The dimensionless kinetic energy T satisfies

$$T = \frac{1}{2}(r_1(1 + s_1)\dot{s}_1^2 + r_2(1 + s_2)\dot{s}_2^2 + r_b d u_b^2),$$

where u_b is the non-dimensional flow speed in the horizontal chamber. Conservation of mass requires that $r_1 s_1 = -r_2 s_2$ and additionally that $r_1 \dot{s}_1 = -r_2 \dot{s}_2 = -r_b u_b$ for all $t > 0$. Using these continuity equations, s_1 and \dot{s}_1 are eliminated and the Lagrangian $\mathbf{L} \equiv T - V$ is calculated in terms of s_2 . On letting $s_2 = s$ and applying Lagrange's equation

$$\frac{d}{dt} \left[\frac{\partial \mathbf{L}}{\partial \dot{s}} \right] = \frac{\partial \mathbf{L}}{\partial s},$$

we obtain

$$\ddot{s}(1 + as + \kappa) + \frac{1}{2}a\dot{s}^2 + s = 0, \quad (2.1)$$

where

$$a = 1 - \frac{r_2}{r_1} \quad (2.2)$$

and

$$\kappa = \frac{(r_1 + r_2)(1 - a)d}{r_b(2 - a)^2}. \quad (2.3)$$

Equations (2.1)–(2.3) are central to the calculations in this paper and will be referred to throughout. Equation (2.2) defines the parameter a that is a measure of the asymmetry of the columns, with $0 \leq a < 1$. When $r_1 = r_2$, we have $a = 0$ and hence (2.1) reduces to a linear differential equation describing oscillations in a symmetric U-tube. In that case, the solutions are sinusoidal and have dimensionless period $2\pi\sqrt{1 + \kappa}$. However, when $r_1 \gg r_2$ and hence $a \approx 1$, the nonlinearities in (2.1) become significant. While there is apparently no direct mechanical analogy to (2.1), as discussed in §1, Bernoulli (1738) noted that an asymmetric liquid oscillator can be considered equivalent in certain respects to a simple pendulum whose length depends on the asymmetry a , as given here.

The parameter κ defined by (2.3) is a function of the asymmetry parameter and arises through a consideration of fluid motion in the horizontal chamber. One should note that different configurations of the U-tube can have the same value of κ . In §2c the special case of $\kappa = 0$ is considered before non-zero values are discussed.

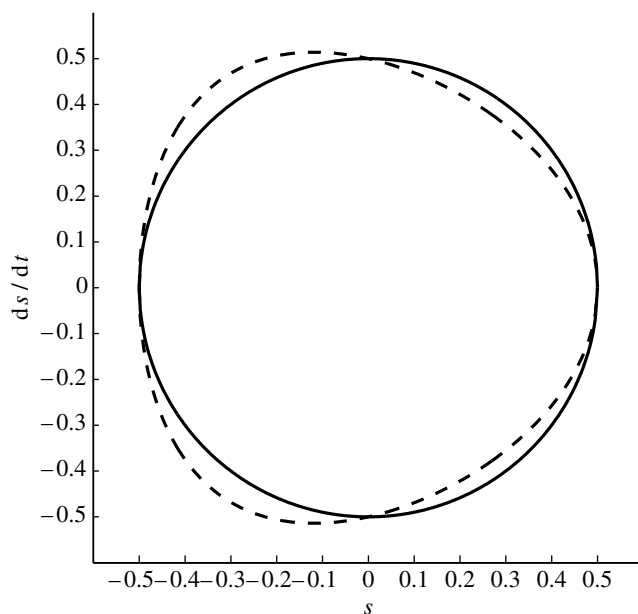


Figure 2. Phase plane of U-tube with $\kappa=0$ for $S_0=0.5$: $a=0.0$ (solid line) and $a=0.95$ (dashed line).

(b) *Phase-plane analysis*

Equation (2.1) may be rewritten as a system of two first-order differential equations

$$\dot{s} = y, \quad (2.4)$$

$$\dot{y} = \frac{-\frac{1}{2}ay^2 - s}{1 + as + \kappa}. \quad (2.5)$$

On combining equations (2.4) and (2.5) we obtain

$$\frac{dy}{ds} = -\frac{\frac{1}{2}ay^2 + s}{y(1 + as + \kappa)}$$

and hence,

$$\frac{d}{ds}[\dot{s}^2(1 + as + \kappa)] = -2s,$$

which describes curves in the phase plane (s, \dot{s}) and has solutions

$$\dot{s} = \pm \sqrt{\frac{S_0^2 - s^2}{1 + as + \kappa}}, \quad (2.6)$$

through the point $(S_0, 0)$. Equation (2.6) is plotted in figure 2 for a symmetric U-tube ($a=0$) and a highly asymmetric U-tube ($a=0.95$) for the particular case of $\kappa=0$ (see §2c).

Rearranging (2.6) and integrating over half an oscillation cycle gives the period τ of the oscillation as

$$\tau = 2 \int_{-S_0}^{S_0} \sqrt{\frac{1 + as + \kappa}{S_0^2 - s^2}} ds = 4\sqrt{1 + \kappa + aS_0} E(q), \tag{2.7}$$

where

$$q = \sqrt{\frac{2aS_0}{1 + \kappa + aS_0}},$$

and $E(q)$ is the complete elliptic integral of the second kind, namely (e.g. Gradshteyn & Ryzhik 2000)

$$E(q) = \int_0^{\pi/2} \sqrt{1 - q^2 \sin^2 u} du.$$

Equation (2.7) is evidence that the period of liquid oscillation in the U-tube is a function of the asymmetry parameter a . Furthermore, when $a > 0$ the frequency also depends on the initial displacement. A similar dependence was found by Craik & Hirata (2003) for liquid oscillations in three identical connected columns. The effect of initial displacement on oscillation frequency is in contrast with a symmetric U-tube, where the frequency of oscillation is independent of the displacement (as confirmed by setting $a = 0$ in (2.7)).

(c) Frequency variation ($\kappa = 0$)

The effect of varying the asymmetry of the columns can be isolated by considering the special case of $\kappa = 0$. This corresponds physically to a U-tube in which $r_b \gg d$. Flow speeds in the horizontal chamber are then small when compared with those in the vertical columns. The closed-form expression given in (2.7) does not provide a clear indication of how the period varies with the asymmetry. In this section, a more usable relationship between these quantities is derived via a Poincaré–Lindstedt perturbation analysis of the equation of motion (2.1).

We assume initially that the asymmetry parameter is small ($a \ll 1$), i.e. the vertical columns are almost equal in width. We define $\tau = \omega t$, where ω is the natural angular frequency, and substitute in (2.1) to obtain

$$\omega^2 \ddot{s}(1 + as) + \omega^2 \frac{1}{2} a \dot{s}^2 + s = 0, \tag{2.8}$$

with $s = s(\tau)$ and the derivatives now with respect to τ . We seek solutions of (2.8) of the form

$$s = s_0 + as_1 + a^2 s_2 + \dots, \tag{2.9}$$

$$\omega = \omega_0 + a\omega_1 + a^2 \omega_2 + \dots. \tag{2.10}$$

It is assumed that the fluid is initially displaced by an amount S_0 and starts from rest. The appropriate initial conditions are therefore

$$\begin{aligned} s_0 &= S_0 & \dot{s}_0 &= 0, \\ s_i &= 0 & \dot{s}_i &= 0, \quad i = 1, 2, \dots \end{aligned}$$

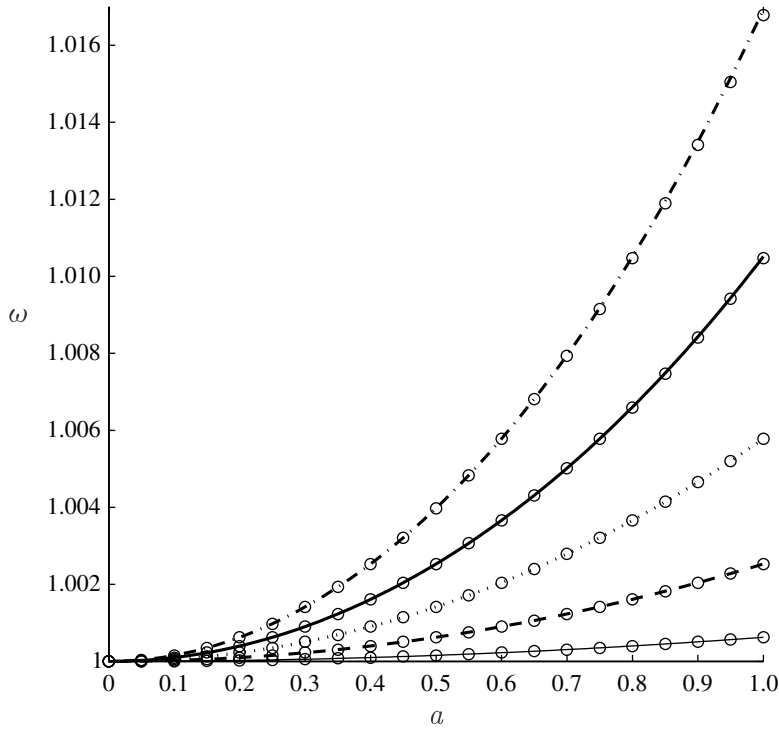


Figure 3. Variation of natural frequency with asymmetry for $\kappa = 0$. Closed-form solution (from equation (2.7), lines) and asymptotic solution (from equation (2.11), circles). $S_0 = 0.1$ (thin solid line), $S_0 = 0.2$ (dashed line), $S_0 = 0.3$ (dotted line), $S_0 = 0.4$ (thick solid line) and $S_0 = 0.5$ (dash-dotted line).

Expressions (2.9) and (2.10) are substituted into (2.8) and the coefficients of the powers of a are compared. The Poincaré–Lindstedt analysis is a standard but lengthy procedure and the details are omitted. For similar calculations refer to [Jordan & Smith \(1997\)](#). In this manner, an approximate expression for the dimensionless angular frequency ω is found to be

$$\omega = 1 + \frac{S_0^2}{16} a^2 + \frac{19S_0^4}{1024} a^4 + O(a^6) \tag{2.11}$$

An approximation for $s(\tau)$ is calculated in a similar manner, namely

$$\begin{aligned} s(\tau) = & S_0 \cos \tau + \frac{S_0^2}{4} (1 - \cos 2\tau)a - \frac{7S_0^3}{64} (\cos \tau - \cos 3\tau)a^2 \\ & + \frac{S_0^4}{384} (15 + 8 \cos 2\tau - 23 \cos 4\tau)a^3 \\ & - \frac{5S_0^5}{12\,288} (79 \cos \tau + 12 \cos 3\tau - 91 \cos 5\tau)a^4 \\ & + \frac{S_0^6}{245\,760} (3600 + 2485 \cos 2\tau - 16 \cos 4\tau - 6069 \cos 6\tau)a^5 + O(a^6). \end{aligned}$$

The above procedure is valid when $a \ll 1$. However, equation (2.11) is in fact accurate for larger values of a . This is demonstrated in [figure 3](#), where the angular frequency ω as calculated using the asymptotic expression (2.11) and the

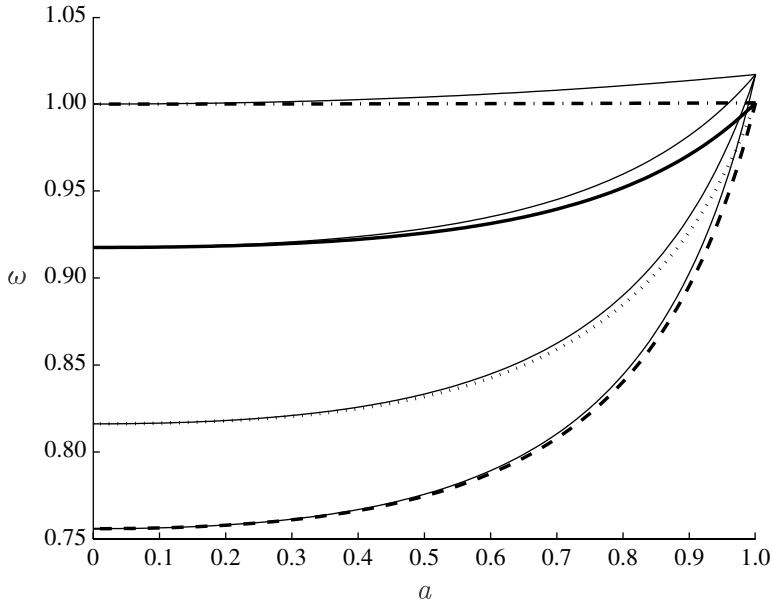


Figure 4. Frequency as a function of asymmetry for $r_1 + r_2 = 0.429$, $d = 1$. $S_0 = 0.1$ with $r_b = 0.143$ (dashed line), $r_b = 0.214$ (dotted line), $r_b = 0.571$ (solid line), $r_b \gg d$ (dash-dotted line) and $S_0 = 0.5$ (thin solid lines).

closed-form expression (2.7) is plotted as a function of a for different values of S_0 . In all cases, (2.11) gives a high level of agreement with (2.7). Even for extreme values when $a \approx 1$, the maximum relative error is only 0.015%.

(d) Frequency variation ($\kappa > 0$)

The §2c gives an insight as to how the angular frequency varies with the asymmetry parameter for $\kappa = 0$. However, we ultimately aim to compare our theory with experimental results, and the configuration of apparatus required to have $\kappa \approx 0$ is physically difficult to build and would not be representative of the general design of a TLCd. It is therefore essential to consider the effect of $\kappa > 0$ in the model.

For any given value of asymmetry a , the height r_b of the horizontal chamber controls the value of κ in (2.3) if both d and $r_1 + r_2$ remain constant. Although similar variation of κ can be obtained by varying these latter parameters, adjusting r_b is the simplest to reproduce experimentally. Figure 4 shows the angular frequency of oscillation calculated from (2.7) as a function of asymmetry for different values of r_b . This example uses $d = 1$, $r_1 + r_2 = 0.429$ and $r_b = 0.143$ values that will become significant later when the experimental results are presented in §4. It is clear from figure 4 that the angular frequency is most sensitive to changes in asymmetry when r_b is small, in which case the angular frequency is less sensitive to the initial displacement of fluid. Initiating an oscillation with a precise initial displacement is difficult in practice. Therefore, these results suggest that for experimental (and perhaps also

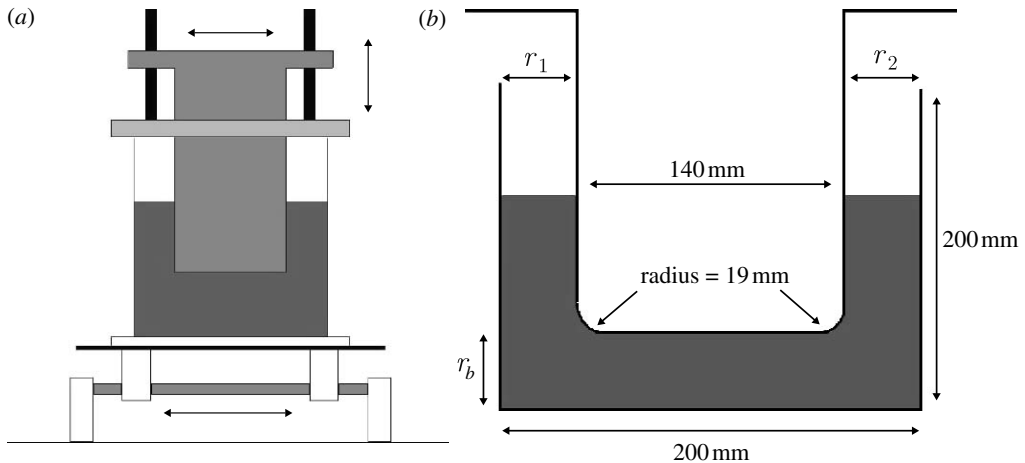


Figure 5. Schematic of experimental apparatus: (a) overall configuration and (b) dimensions of tank and insert.

practical) purposes a horizontal chamber with a small height-to-length ratio is best for investigating the role of asymmetry in a U-tube. This idea is discussed further in §4a.

3. Experimental apparatus

The experimental configuration is shown schematically in figure 5. A cubic Perspex tank of 200 mm interior length is sat on a table that could move horizontally on linear bearings. The tank supported a PVC insert of 140 mm width that spanned the tank and formed the inner walls of the U-tube. The insert was moved horizontally and vertically by two independent lead screws. The horizontal displacement was measured by micrometer to an accuracy of 0.01 mm. The vertical displacement was measured against a graduated scale attached to the outside of the Perspex tank, with an accuracy of 0.2 mm. The corners of the insert were rounded as shown in figure 5. This was done to minimize any streamline separation and hence ensure that the flow remained locally parallel to the boundaries. An optimal radius of curvature of 19.0 mm was found by means of finite-element simulations of steady flow through the domain. However, as will be discussed in §4a, this method of minimizing separation is only effective for chamber heights below approximately 20 mm. Once the chamber becomes taller than this, the flow separates regardless of the corner profile.

Oscillatory motion of the table was driven by a Scotch yoke mechanism rotated by a stepper motor via a 10 : 1 reduction gearbox. The frequency of the sinusoidal translation of the table could be set in the range between 0 and 2 Hz with a stability of better than 0.2%. The amplitude of translation was set manually by means of a lead screw running through a radial offset bearing. One turn of the screw corresponded to a change of forcing amplitude of approximately 0.35 mm. The stroke amplitude was preset before each experiment and was measured using a dial test indicator to an accuracy of 0.01 mm in the range between 0 and 20 mm.

The working fluid that was used in all the experiments reported here was water at room temperature. This is consistent with previous experimental work in this area (e.g. Hitchcock *et al.* 1997*a,b*). A small quantity (approx. 0.001% per volume) of wetting agent was added to reduce surface tension and to increase the mobility of the contact lines on the inner surfaces of the device. The equilibrium depth of the fluid was kept constant at 140 mm, the maximum height of the horizontal channel was 60 mm, and the liquid in the columns to oscillate with a maximum displacement of approximately 55 mm. The experiments were observed by eye in real time and by means of video recordings taken at a rate of 25 Hz. The free-surface displacements were measured against the graduated scale on the tank to an accuracy of 0.2 mm.

4. Results

(a) *Tuning characteristics*

A comparison between the theoretical formulation and the experimental system was made for the variation of the natural frequency with changes to the geometry of the flow domain. A series of experiments were performed over a range of asymmetry a for four different values of horizontal chamber height r_b . The large-amplitude oscillations of the liquid were driven by moving the tank horizontally at frequencies close to resonance before halting the tank motion and allowing the fluid to oscillate freely. The subsequent displacement of the free surface in the narrower column was allowed to decay to a scaled, dimensionless value of approximately 0.2, that being sufficient to ensure that any residual influence of the initial forcing had passed. The time taken for 10 complete oscillations was then recorded. The process was run thrice to obtain an accurate mean value for the oscillation frequency. The experimental results are plotted as symbols in figure 6. Also plotted are the loci of natural frequencies obtained from (2.7) for the same four values of r_b (and hence κ) for the case of $S_0 = 0.2$.

The experimental results in figure 6 show the same qualitative variation of frequency with asymmetry and chamber height as those predicted theoretically for the undamped autonomous system. However, the extent of agreement is clearly dependent on the choice of chamber height r_b . The best agreement is for $r_b = \tilde{r}_b = 0.143$ (which corresponds to a dimensional height of 20 mm). For $r_b < \tilde{r}_b$, the experimental values fall moderately below those of the numerical predictions, indicating that the liquid oscillations are slower than expected. This observation can be attributed to the increased influence of viscosity on the flow in the horizontal chamber, an effect that was not incorporated in the theoretical model. However, for $r_b > \tilde{r}_b$ the extent of disagreement becomes considerable, with the experimental values now exceeding those predicted theoretically. Flow visualization experiments and finite-element simulations of steady flow through the domain revealed that for these taller connecting chambers the flow inevitably separates on departure from the descending column. This drives secondary circulations within the horizontal chamber, and the overall flow is far from being the uniform horizontal flow that is assumed in the theory. Hence, throughout the remainder of the study the chamber height was held constant at $r_b = 0.143$ to satisfy the assumptions made in the theoretical modelling.

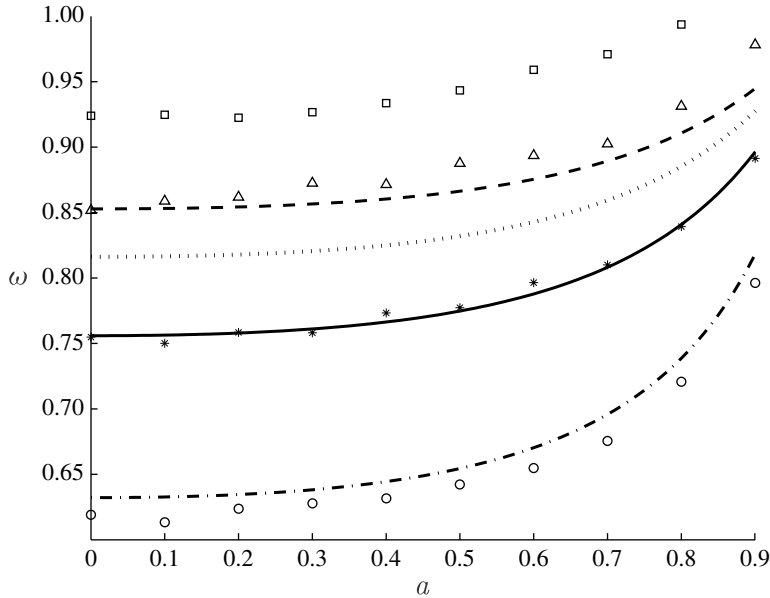


Figure 6. Experimental points and numerical plots of frequency as a function of asymmetry for horizontal chambers of height $r_b = 0.0714$ (circles, dash-dotted line), 0.143 (asterisks, solid line), 0.214 (triangles, dotted line), 0.286 (squares, dashed line).

(b) *Incorporation of damping and forcing*

The theoretical equation of motion (2.1) is undamped and autonomous. However, in order to generate a numerical model against which experimental results could be compared, it was necessary to modify (2.1) to include frictional and forcing effects.

Firstly, a damping term was sought that would best reproduce the decay of oscillations found experimentally. A series of experiments was performed with $a=0$ and $r_b = 0.143$ in which large-amplitude oscillations of the liquid were driven by moving the tank horizontally at frequencies close to resonance before halting the tank motion and allowing the fluid to oscillate freely. The subsequent displacement of the free surface in one of the columns was plotted from video records once the dimensionless amplitude had decayed to approximately 0.2, that being sufficient to ensure that any residual influence of the initial forcing had passed. Different damping terms ($\beta\dot{s}$, $\beta\dot{s}|\dot{s}|$, $\beta\dot{s}^3$) were added to (2.1) that was integrated numerically in each case and results were compared to the experimental time series. The best agreement was found when the damping term took the form $\beta\dot{s}$ (data not shown). This is significant in as much as it is easy to show that in the absence of a pressure gradient, two-dimensional laminar flow in a uniform channel results in a velocity profile that decays exponentially at a rate that is proportional to the viscosity of the fluid. Thus our empirical choice of damping is in line with that, which is known to occur in channels due to viscous forces.

The external oscillatory motion of the system was modelled by adding a term $F \cos \Omega t$ to the r.h.s. of (2.1). The horizontal motion of the tank leads to a time-dependent acceleration vector acting on the fluid, whose vertical component

remains that due to gravity but which in addition has a non-zero horizontal component. This in turn leads to an inertial forcing term in the full Navier–Stokes equations for the problem, which is equivalent in this study to the additional term in (2.1). Thus, the fully damped and forced equation of motion that was used in the numerical investigations discussed below is

$$\ddot{s}(1 + as + \kappa) + \frac{1}{2}as^2 + \beta\dot{s} + s = F \cos \Omega t. \quad (4.1)$$

The use of a periodic forcing term is mathematically consistent with the method used by engineers to model the external excitation of a tall building fitted with a TLCD system (Kwok *et al.* 1997). More detailed information on the motion of tall buildings is given by Jeary (1996), Satake & Yokota (1996) and Tamura *et al.* (2001*b*).

(c) *Resonant characteristics* ($\beta > 0$)

We assume on the basis of all that has been discussed previously that (4.1) is an accurate description of the liquid-column oscillator when $r_b = 0.143$. Thus, it is possible to use (4.1) as a vehicle for investigating the oscillatory response to resonant forcing akin to the conditions that pertain in a practical device that has been tuned to the natural frequency of the supporting structure.

Equation (4.1) can be solved exactly in the symmetric system, where $a=0$ (e.g. Takwale & Puranik 1985). The solution in the underdamped regime of $\beta < 2\sqrt{1+\kappa}$ is

$$s(t) = S \exp\left(-\frac{\beta t}{2(1+\kappa)}\right) \sin\left(\frac{\sqrt{1-\frac{\beta^2}{4}+\kappa}}{1+\kappa}t + \phi\right) + A \cos(\Omega t - \theta), \quad (4.2)$$

where S and ϕ are constants related to the state of the system at $t=0$. The other constants A and θ are given by

$$A = \frac{F}{\sqrt{(1-(1+\kappa)\Omega^2)^2 + \beta^2\Omega^2}} \quad (4.3)$$

and

$$\tan \theta = \frac{\beta\Omega}{1-(1+\kappa)\Omega^2}. \quad (4.4)$$

The first term in (4.2) describes the transient of the solution, which decays to zero over a time scale that is determined by the damping coefficient β . The second term corresponds to the sustained part of the solution, which has the same angular frequency Ω as the external forcing and an amplitude A that is given by (4.3). The amplitude reaches a maximum value of $(F\sqrt{1+\kappa})/\beta$ when the forcing frequency Ω equals the natural frequency $\omega_0 = 1/\sqrt{1+\kappa}$. The reciprocal variation of ω_0 with κ means that a longer horizontal chamber (and hence a larger value of κ ; see (2.3)) will result in smaller oscillations in the columns. Equation (4.4) describes the phase difference between the fluid oscillations and the applied forcing. If Ω is increased from 0 to ω_0 then θ increases from 0 to $\pi/2$. As Ω is increased beyond resonance, θ tends to π . The change in phase is also influenced by β . In highly damped systems the transition of θ from 0 to π is relatively smooth; however, it becomes more abrupt as the damping is decreased. Further reading on this transition can be found in Takwale & Puranik (1985).

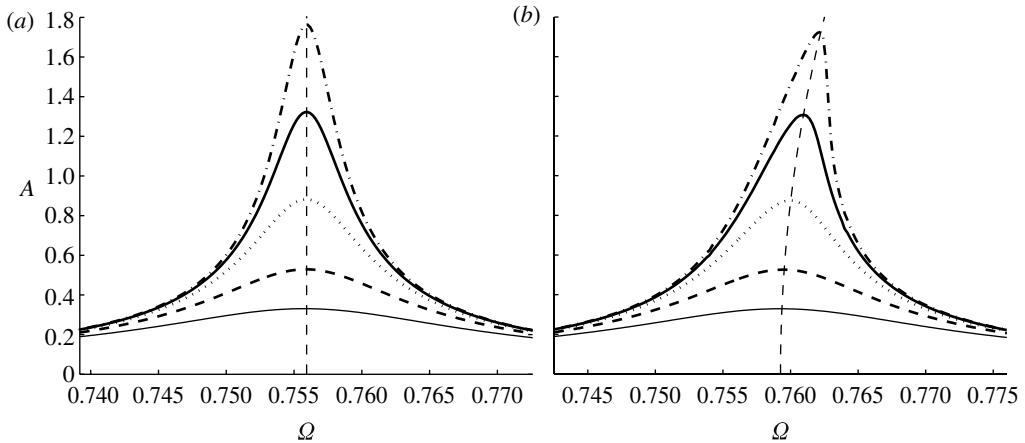


Figure 7. Resonant response of oscillation amplitude A with forcing frequency Ω for $r_1 + r_2 = 0.429$, $r_b = 0.143$, $d = 1$, $F = 0.01$ and $\beta = 0.04$ (thin solid line), $\beta = 0.025$ (dashed line), $\beta = 0.015$ (dotted line), $\beta = 0.01$ (thick solid line) and $\beta = 0.0075$ (dash-dotted line). (a) Symmetric ($a = 0$) and (b) asymmetric ($a = 0.25$). The dashed lines tracking the maximum resonant amplitudes are obtained from equation (2.7) with $\Omega = 2\pi/\tau$ and $S_0 = A$.

When $a > 0$, (4.1) is nonlinear and does not admit an exact analytical solution. Instead, (4.1) was integrated numerically within MATLAB using standard fourth-order Runge–Kutta methods with double-precision accuracy and time-step checking. The algorithm was tested for the case $a = 0$ by comparison with the exact solution (4.2)–(4.4), and was found to be accurate to within the limits of numerical precision.

Resonance curves obtained from (4.1) are shown in figure 7 for two values of the asymmetry parameter a , namely $a = 0$ and 0.25 . In both cases, the damping parameter β was set to several different values in the underdamped regime. The curves in figure 7a for $a = 0$ were obtained directly from (4.3) with $\kappa = 0.75$. The linearity of the system when $a = 0$ is evident from the symmetric distribution of the oscillation amplitude about the natural frequency. The reciprocal variation of the maximum amplitude with damping is also clearly evident. The curves in figure 7b for $a = 0.25$ were obtained by numerical integration. Despite the inclusion of asymmetry in (4.1), many of the features of (4.2)–(4.4) were found in the numerical solutions. As before, there was a transient with a duration dependent on the damping, and a sustained solution with the same frequency as the applied forcing and with an amplitude that exhibited resonance with variation of Ω . However, the main difference from $a = 0$ is the skewed asymmetric nature of the resonance curves. This becomes more pronounced as the damping coefficient β is decreased and hence the maximum amplitude A_{\max} increases. A similar nonlinear resonance is known to exist for periodically forced shallow fluid layers (Kobine in press). In that case, the resonance curves are skewed to higher or lower frequencies depending on whether the layer depth is less than or greater than a critical depth.

Equation (2.7) allows the natural frequency $\omega_0 = 2\pi/\tau$ of free oscillations of amplitude $S_0 = A$ to be calculated for a particular value of asymmetry a . The variation of natural frequency with oscillation amplitude is indicated in figure 7.

When $a=0$, the natural frequency is independent of amplitude and takes the value $\omega_0 = 1/\sqrt{1+\kappa} = 0.7559$ as shown in figure 7a. However, when $a>0$ the natural frequency of the system increases with oscillation amplitude. As can be seen in figure 7b, the variation described by (2.7) for $a=0.25$ gives an accurate prediction of the forcing frequency at which the maximum resonant response was found numerically.

(d) *Resonant characteristics ($\beta=0$)*

The above discussion for $\beta > 0$ assumed that all initial transient behaviour had decayed to leave a persistent long-term response to the imposed forcing. However, in any practical TLCD device the initial response of the liquid to an imposed motion will be critical, as this is when the motion of the structure is greatest and so is likely to cause the most damage. Thus it is of interest to study the interaction between the free and forced liquid motion in the present mathematical model. This can be done most conveniently by setting $\beta=0$ to prevent any decay of the free component.

The case of $\beta=0$ for the symmetric system ($a=0$) can be studied analytically by means of (4.2). Setting realistic initial conditions of $s(0) = \dot{s}(0) = 0$ leads to values for S and ϕ of $-A$ and $\pi/2$, respectively. Thus, (4.2) becomes

$$s(t) = -A(\cos \omega_0 t - \cos \Omega t) = 2A \sin\left(\frac{\omega_0 - \Omega}{2} t\right) \sin\left(\frac{\omega_0 + \Omega}{2} t\right), \quad (4.5)$$

where

$$A = \frac{\omega_0^2 F}{|\omega_0^2 - \Omega^2|}, \quad (4.6)$$

and $\omega_0 = 1/\sqrt{1+\kappa}$. Equations (4.5) and (4.6) represent a modulated sinusoidal oscillation in which both the modulation period and amplitude tend to infinity as the forcing frequency Ω approaches the natural frequency ω_0 . A convenient way to study the behaviour as Ω is varied through ω_0 is to take Poincaré sections in the (s, \dot{s}) phase space by sampling the solution and its derivative at times $t = 2\pi n/\Omega$ for $n=0, 1, 2, \dots, N$ (e.g. Thompson & Stewart 1986). This is equivalent to sampling the state of the system each time the imposed forcing reaches its positive maximum value. A set of representative Poincaré sections is shown in figure 8a for $F=0.01$ and the values of Ω below and above the natural frequency of $\omega_0 = 0.7559$. When $\Omega < \omega_0$, the Poincaré sections are closed loops in the right half of the phase space, indicating that the phase of the liquid motion is allied to that of the forcing. As Ω approaches ω_0 the size of the loops grows, becoming infinite at $\Omega = \omega_0$. When $\Omega > \omega_0$, the loops become finite in size once again but are now in the left half of the phase space, indicating an opposition between the forcing and response phases. It is interesting to note that by viewing the dynamics in terms of Poincaré sections instead of the more conventional time-series approach, it becomes possible to see both the amplitude and phase information simultaneously.

For the general case $a>0$, again no closed-form solution of (4.1) exists and so we used numerical integration as detailed above. Solutions to the asymmetric system, with $a=0.25$, were obtained and values of (s, \dot{s}) returned at times $t = 2\pi n/\Omega$ for $n=0, 1, 2, \dots, N$. Poincaré sections for $a=0.25$ and various values of the forcing frequency Ω are shown in figure 8b for a fixed forcing amplitude of

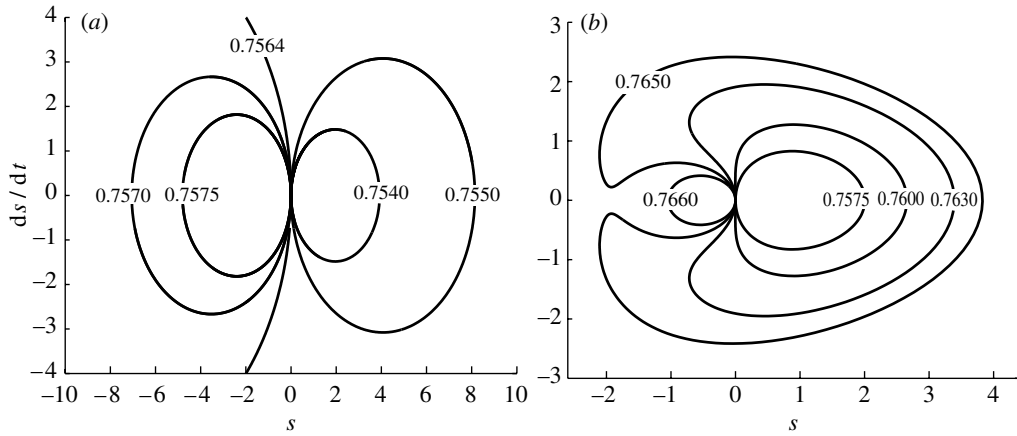


Figure 8. Poincaré sections of undamped resonant response for $r_1 + r_2 = 0.429$, $r_b = 0.143$, $d=1$ and $F=0.01$: (a) $a=0$ and (b) $a=0.25$. Individual Poincaré sections are labelled with the corresponding dimensionless forcing frequency Ω .

$F=0.01$. As Ω is increased, the response is initially qualitatively the same as that for $a=0$, with closed loops in the right half of the phase space. However, as the overall response amplitude increases, the effect of nonlinearity becomes more significant and causes the Poincaré sections to extend over into the left half of the plane. The limit of this extension is when the two leftward protruding lobes of the Poincaré section meet on the $\dot{s}=0$ axis, after which the spade-like structure collapses and the points fall instead on regular elliptical loops but now in the left half of the phase space.

It is significant that, unlike the $a=0$ case, the nonlinearities present when $a>0$ prevent the occurrence of a resonant singularity in the amplitude regardless of the fact that the damping is equal to zero. It is also worth noting that the natural frequency of a TLCD is typically set to within 3% of the natural frequency of the first mode of oscillation of the building (e.g. Kwok *et al.* 1997). However, the transition sequences illustrated in figure 8 take place over less than 1% of the mean frequency values. This suggests that higher tuning tolerances would be required in a practical device that relied on asymmetry to set the natural frequency of the liquid oscillations.

5. Conclusion

The most significant finding of the present study is that the degree of asymmetry of a generalized liquid-column oscillator has a role to play in determining the natural frequency of free oscillations of the liquid volume. Hence it offers a method of tuning the response frequency of practical liquid-column damping devices in addition to the accepted methods of altering the equilibrium depth and varying the height of the connecting chamber. While the latter method has the advantage over the former of not requiring liquid to be pumped to or from the device, it nevertheless presents significant challenges to any attempt to model the internal dynamics due to the problems of increased viscous damping at the smallest chamber heights and flow separation if the chamber height is too large.

The introduction of asymmetry to the configuration allows the liquid volume to remain constant and the chamber height to be optimized with respect to boundary layer and separation effects, while retaining the facility to control oscillation frequency by means of a geometrical alteration that would be easy to implement in a practical device and that is amenable to being modelled mathematically.

The above theoretical description of the problem has allowed the fundamental dynamical properties of this type of flow configuration to be exposed in a manner that could be used in the design of applicable systems. Asymmetry between the two vertical columns in terms of their widths being unequal contributes a nonlinear term to the ordinary differential equation that governs the motion of the liquid volume. In the case of free oscillations, this equation has been solved by means of phase-plane analysis to give an exact analytical expression for the natural frequency in terms of the asymmetry and the chamber height. However, a more useable and highly accurate approximation for the same variation for large chamber heights was derived by means of a Poincaré–Lindstedt perturbation analysis. Crucially, the variation of frequency with asymmetry for realistic chamber heights was tested against experimental data. This confirmed the predictions of the theoretical model, but with an important caveat regarding the choice of chamber height.

Finally, insights have been gained into the nonlinear resonant response of the asymmetric system to external forcing by means of numerical investigation of the damped non-autonomous version of the equation of motion. The long-term amplitude response shows the familiar skewed distribution equivalent to hard-spring behaviour. However, the most novel results to emerge relate to the probable initial response of the liquid volume to a periodic external excitation that was explored through the use of being able to set the damping coefficient in the model to zero. The information about the amplitude and phase of the resulting oscillations was combined through the use of Poincaré sections in phase space. Thus, a standard technique from classical nonlinear dynamics was used to good effect in the analysis of a problem with important practical consequences in the field of structural engineering.

The authors are grateful to Prof. A. Craik for extremely useful discussions in the early stages of this project. M.J.S. was funded by an EPSRC Doctoral Training grant.

References

- Bernoulli, D. 1738 *Hydrodynamica*. Argentorati (Strassburg), Germany: Johann Reinhold Dulsecker.
- Chen, W. & Scawthorn, C. 2003 *Earthquake engineering handbook*. Boca Raton, FL: CRC Press.
- Craik, A. D. D. & Hirata, K. 2003 Nonlinear oscillations in three-armed tubes. *Eur. J. Fluid Mech.* **22**, 3–26.
- Field, S. B. & Martin, J. P. 1976 Comparative effects of U-tube and free surface type passive roll stabilisation systems. *Nav. Archit.* **2**, 73–92.
- Gao, H., Kwok, K. C. S. & Samali, B. 1999 Characteristics of multiple tuned liquid column dampers in suppressing structural vibration. *J. Eng. Struct.* **21**, 316–331. (doi:10.1016/S0141-0296(97)00183-1)
- Gradshteyn, I. S. & Ryzhik, I. M. 2000 *Table of integrals, series & products*, 6th edn. London, UK: Academic Press.

- Hitchcock, P. A., Kwok, K. C. S., Watkins, R. D. & Samali, B. 1997*a* Characteristics of liquid column vibration absorbers (LCVA)—part I. *J. Eng. Struct.* **19**, 126–134. (doi:10.1016/S0141-0296(96)00042-9)
- Hitchcock, P. A., Kwok, K. C. S., Watkins, R. D. & Samali, B. 1997*b* Characteristics of liquid column vibration absorbers (LCVA)—part II. *J. Eng. Struct.* **19**, 135–144. (doi:10.1016/S0141-0296(96)00044-2)
- Holmes, J. D. 1995 Auxiliary damping systems for mitigation of wind-induced vibration. *J. Eng. Struct.* **17**, 608–621. (doi:10.1016/0141-0296(95)00029-7)
- Holmes, J. D. 2001 *Wind loading of structures*. London, UK: Spon Press.
- Jeary, A. P. 1996 The description and measurement of nonlinear damping in structures. *J. Wind Eng. Ind. Aerodyn.* **59**, 103–114. (doi:10.1016/0167-6105(96)00002-5)
- Jordan, D. W. & Smith, P. 1997 *Nonlinear ordinary differential equations*, 3rd edn. Oxford, UK: University Press.
- Kibble, T. W. B. & Berkshire, F. H. 2004 *Classical mechanics*, 5th edn. London, UK: Imperial College Press.
- Kobine, J. J. In press. Nonlinear resonant characteristics of shallow fluid layers. *Phil. Trans. R. Soc. A*. (doi:10.1098/rsta.2007.2134)
- Kwok, K. C. S., Xu, Y. L. & Samali, B. 1991 Control of wind-induced vibrations of tall structures by optimized tuned liquid column dampers. In *Proc. Asian Pac. Conf. Comput. Mech.*, pp. 249–254.
- Kwok, K. C. S., Samali, B. & Gao, H. 1997 Optimization of tuned liquid column dampers. *J. Eng. Struct.* **19**, 476–486. (doi:10.1016/S0141-0296(96)00099-5)
- Plate, E. J. & Kiefer, H. 2001 Wind loads in urban areas. *J. Wind Eng. Ind. Aerodyn.* **89**, 1233–1256. (doi:10.1016/S0167-6105(01)00159-3)
- Ribakov, Y., Gluck, J. & Reinhorn, A. M. 2001 Active viscous damping system for control of MDOF structures. *J. Earthquake Eng. Struct. Dyn.* **30**, 195–212. (doi:10.1002/1096-9845(200102)30:2<195::AID-EQE4>3.0.CO;2-X)
- Sakamoto, D., Oshima, N. & Fukuda, T. 2001 Tuned sloshing damper using electro-rheological fluid. *Smart Mater. Struct.* **10**, 963–969. (doi:10.1088/0964-1726/10/5/312)
- Satake, N. & Yokota, H. 1996 Evaluation of vibration properties of high-rise steel buildings using data of vibration tests and earthquake observations. *J. Wind Eng. Ind. Aerodyn.* **59**, 265–282. (doi:10.1016/0167-6105(96)00011-6)
- Takwale, R. G. & Puranik, P. S. 1985 *Introduction to classical mechanics*. New Delhi, India: Tata McGraw-Hill.
- Tamura, Y. 1998 Application of damping devices to suppress wind-induced responses of buildings. *J. Wind Eng. Ind. Aerodyn.* **74–76**, 49–72. (doi:10.1016/S0167-6105(98)00006-3)
- Tamura, Y., Hibi, K. & Kikuchi, H. 2001*a* Extreme wind pressure distributions on low-rise building models. *J. Wind Eng. Ind. Aerodyn.* **89**, 1635–1646. (doi:10.1016/S0167-6105(01)00153-2)
- Tamura, Y., Yasui, H. & Marukawa, H. 2001*b* Non-elastic responses of tall steel buildings subjected to across-wind forces. *Wind Struct.* **4**, 147–162.
- Thompson, J. M. T. & Stewart, H. B. 1986 *Nonlinear dynamics & chaos*. New York, NY: Wiley.
- Xu, Y. L., Samali, B. & Kwok, K. C. S. 1992 Control of along-wind response of structures by mass and liquid dampers. *J. Mech. Eng.* **118**, 20–39. (doi:10.1061/(ASCE)0733-9399(1992)118:1(20))